*Computational Star Formation*
*Proceedings IAU Symposium No. 270, 2011*
*J. Alves, B.G. Elmegreen, J. M. Girart & V. Trimble, eds.*

doi:10.1017/S1743921311000585

# The interaction of an HII region with a fractal molecular cloud

**Steffi Walch[1], Ant Whitworth[1], Thomas Bisbas[1,2], Richard Wünsch[1,2] and David Hubber[3]**

[1]School of Physics & Astronomy, Cardiff University, UK
emails: Stefanie.Walch@astro.cf.ac.uk, Anthony.Whitworth@astro.cf.ac.uk

[2]Czech Academy of Sciences, Prague, Czech Republic
emails: Thomas.Bisbas@astro.cf.ac.uk, richard@wunsch.cz

[3]Department of Physics & Astronomy, Sheffield University, UK
email: D.Hubber@sheffield.ac.uk

**Abstract.** We describe an algorithm for constructing fractal molecular clouds that obeys prescribed mass and velocity scaling relations.The algorithm involves a random seed, so that many different realisations corresponding to the same fractal dimension and the same scaling relations can be generated. It first generates all the details of the density field, and then position the SPH particles, so that the same simulation can be repeated with different numbers of particles to explore convergence. It can also be used to initialise finite-difference simulations. We then present preliminary numerical simulations of HII regions expanding into such clouds, and explore the resulting patterns of star formation. If the cloud has low fractal dimension, it already contains many small self-gravitating condensations, and the principal mechanism of star formation is radiatively driven implosion. This results in star formation occurring quite early, throughout the cloud. The stars resulting from the collapse and fragmentation of a single condensation are often distributed in a filament pointing radially away from the source of ionising radiation; as the remainder of the condensation is dispersed, these stars tend to get left behind in the HII region. If the cloud has high fractal dimension, the cloud does not initially contain dense condensations, and star formation is therefore delayed until the expanding HII region has swept up a sufficiently massive shell. The shell then becomes gravitationally unstable and breaks up into protostars. In this collect-and-collapse mode, the protostars are distributed in tangential arcs, they tend to be somewhat more massive, and as the expansion of the shell stalls they move ahead of the ionisation front.

**Keywords.** HII regions, molecular clouds, ionisation fronts, triggered star formation

## 1. Introduction

This project is aimed at understanding the role of feedback from massive stars in star-forming molecular clouds, i.e. how, and under what circumstances, massive stars may trigger, or accelerate, or inhibit, or terminate star formation. In particular, we are concerned here with the effect of an HII region expanding into a molecular cloud, and the relative importance of (i) *radiatively-driven implosion* (i.e. where the action of the ionisation front, and the shock front that precedes it, is to compress pre-existing condensations and trigger their collapse) and (ii) *collect-and-collapse* (i.e. where the HII region sweeps up a dense shell, which eventually becomes sufficiently massive to fragment and collapse). These two mechanisms are expected to deliver rather distinct patterns of star formation, and there may also be differences in the properties of the stars they produce (e.g. mass function, binary statistics, velocity dispersion). We are therefore investigating, by means of SPH simulations, how the expansion of an HII region into a molecular

cloud is influenced by the cloud having pre-existing fractal substructure. This is a timely project because, in the aftermath of SPITZER, and with the advent of HERSCHEL, we now have a wealth of observational data on star formation at the boundaries of HII regions, against which to test the credibility of our models (e.g. Churchwell *et al.* 2004; Deharveng *et al.* 2009; Koenig *et al.* 2008; Smith *et al.* 2010).

## 2. Initial conditions

We model molecular clouds with a fractal structure, i.e. a nested, self-similar hierarchy of clumps within clumps. This hierarchy is characterised by two parameters, $D$ and $C$. The fractal dimension $D$ determines, for a clump on level $\ell$ of the hierarchy, what fraction $f$ of its volume is occupied by clumps on the next level $(\ell + 1)$. For an octal fractal structure, i.e. one in which each clump can be divided into a maximum of eight subclumps,

$$f \quad = \quad 2^{3-D} \tag{2.1}$$

Thus, if $D = 3$, $f = 1$ and the density distribution inside the clump is smooth. As $D$ is reduced, $f$ decreases, and hence the fraction of a clump's volume that is occupied by subclumps is reduced. We consider values of $D$ in the interval $2.0 < D < 2.8$.

The density contrast $C$ determines the factor by which clumps on level $\ell+1$ are denser than those on level $\ell$. It follows that mass, $M$, scales with linear size, $L$, according to

$$M \quad \propto \quad L^{\chi_{ML}} \, , \qquad \chi_{ML} \quad = \quad 3 \, - \, \log_2(C) \, . \tag{2.2}$$

Kaufmann *et al.* (2010) find $\chi_{ML} = 1.3 \pm 0.1$, and hence we put

$$C \quad = \quad 2^{3-\chi_{ML}} \quad = \quad 3.25 \pm 0.25 \, . \tag{2.3}$$

Once the fractal dimension, $D$, and the density contrast, $C$, are specified, the mass spectrum of clumps is given by

$$\frac{dN}{dM} \quad \propto \quad M^{-\zeta_{NM}} \, , \qquad \zeta_{NM} \quad = \quad \frac{D}{\chi_{ML}} \tag{2.4}$$

(cf. Stutzki *et al.* 1998); and the volume-weighted logarithmic density PDF is given by

$$\frac{dV}{d\ell og(\rho)} \quad \propto \quad \rho^{-\zeta_{V\rho}} \, , \qquad \zeta_{V\rho} \quad = \quad \frac{(3-D)}{\log_2(C)} \quad = \quad \frac{(3-D)}{(3-\chi_{ML})} \, . \tag{2.5}$$

Note that we can also give the clumps bulk velocities, so that the internal velocity dispersion of a clump on level $\ell$ derives from the bulk velocities of the smaller clumps it contains. In this case we have to introduce a third parameter characterising the velocity scaling law (Larson 1981). As with the density contrast, $C$, this parameter is constrained by the observed velocity scaling law. However, in the simulations presented here these velocities are unimportant, and so we neglect them.

We construct fractal clouds by starting with a cubic root cell (the whole computational domain) in which the density is set to a minimum value, $B$. We then divide the root cell into eight approximately, but not exactly, equal subcells, by splitting the root cell first with a single surface orthogonal to one of the Cartesian axes, then splitting the two resulting parts with two surfaces orthogonal to one of the other Cartesian axes, and finally splitting the four resulting parts with four surfaces orthogonal to the remaining Cartesian axis. Next we pick, using random numbers, a subset of $2^D$ of these subcells. These are the fertile subcells, and we therefore increase their densities by a factor of $C$. The remaining $8 - 2^D$ subcells are infertile, and so their densities are unchanged. We

then repeat this process of dividing fertile cells into subcells and picking a subset of the subcells to be fertile; once a cell is identified as being infertile, nothing further happens to it. Since $2^D$ is not in general an integer, we carry forward surplus fertility to the next cell, or the next generation of cells. The process is repeated recursively through a user-specified number of levels (specified with the proviso that the clumps on the lowest level should be resolved by $\gtrsim 50$ SPH particles). In order to get rid of alignments with the Cartesian axes, the subcells within a given cell are rotated about the centre of the parent cell, through three random angles; where necessary particles are wrapped periodically. This algorithm works well for clouds with low fractal dimension, $D \lesssim 2.8$, but breaks down as the fractal dimension approaches 3, because – in this limit – the random rotations create a significant amount of spurious (non-fractal) sub-structure.

The cloud mass and initial radius are fixed at $M_{\rm CLOUD} = 780\,{\rm M}_\odot$ and $R_{\rm CLOUD} = 1\,{\rm pc}$. By fixing the cloud mass and radius, we can easily generate a single-parameter family of clouds by only varying the fractal dimension. However, we should be aware that the density PDF then extends to higher densities in the clouds with lower fractal dimension.

A constant isotropic source of ionising photons, $\dot{\mathcal{N}}_{\rm LyC} = 10^{49}\,{\rm s}^{-1}$, is switched on instantaneously at the centre of the cloud. The temperature of the ionised gas is set to $10^4\,{\rm K}$, and the temperature of the neutral gas is set to $10\,{\rm K}$; the temperature discontinuity across the ionisation front is smoothed over a few smoothing lengths.

## 3. Numerical method

We use the state-of-the-art SPH code SEREN (Hubber *et al.* 2010) to follow the self-gravitating gas dynamics, with between $10^6$ and $10^7$ particles. We use the HEALPix-based algorithm of Bisbas *et al.* (2009) to treat the transport of ionising radiation, with up to 9 levels of refinement, and hence a finest resolution of $\sim 100$ rays per square degree. We neglect the diffuse ionising radiation field, by invoking the On-The-Spot Approximation. Hence, along each ray (represented by the unit vector $\hat{\mathbf{k}}$) the location of the ionisation front ($\mathbf{r}_{\rm IF} = R\hat{\mathbf{k}}$) is given by

$$\int_{r=0}^{r=R} n^2\left(r\hat{\mathbf{k}}\right) r^2\,dr \;=\; \frac{\dot{\mathcal{N}}_{\rm LyC}}{4\,\pi\,\alpha_{\rm B}}\,. \tag{3.1}$$

Here $n$ is the number-density of hydrogen, and $\alpha_{\rm B}$ is the recombination coefficient into excited states only. Sink particles are introduced if the density exceeds $\rho_{\rm SINK} = 10^{-11}\,{\rm g\,cm}^{-3}$ (by which stage a protostellar condensation should be well into its Kelvin-Helmholtz contraction phase), provided various other conditions are met (see Hubber *et al.* 2010). The simulations are extremely well converged, in the sense that almost exactly the same evolution is seen with $10^6$ and $10^7$ SPH particles. Magnetic effects are not included; nor is radiation pressure.

## 4. Results and Conclusions

Fractal clouds appear to offer a promising way of modelling observed molecular clouds with a relatively small number of parameters, and hence of initialising numerical simulations of cloud evolution and star formation. As the fractal dimension decreases from $D = 3$, we move from a regime in which the cloud density is initially uniform to one in which the cloud is, from the outset, highly structured, with many dense compact condensations.

For low fractal dimension, star formation occurs mainly by radiatively driven implosion. Because there is no delay whilst a dense massive shell is swept up, star formation

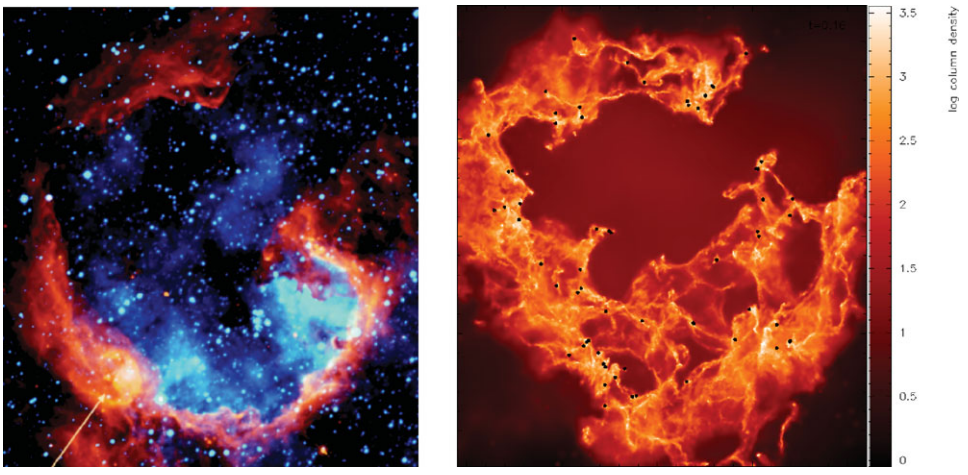


**Figure 1.** Left: RCW 79 observed with Spitzer IRAC 8 $\mu$m image (orange) superimposed on a SuperCOSMOS H$\alpha$ image (turquoise) (credit: Zavagno *et al.* 2006). Right: Column density plot showing the dense shell structure formed when ionising a cloud with $D = 2.8$ for 0.5 Myr.

occurs early (at $t \gtrsim 0.2$ Myr for the cloud parameters given in section 2), and at many different radii, more or less simultaneously. The resulting protostars tend to have random velocities. As their natal envelope is ablated, they get left behind in the HII region.

For high fractal dimension, star formation occurs mainly by the collect-and-collapse mode, therefore later (at $t \gtrsim 0.4$ Myr for this setup) and at larger radius. It creates stars arranged in tangential arcs, and with systematic outwards velocities, so that they tend to move ahead of the ionisation front. Figure 1 (righthand frame) shows one example of a dense, swept-up shell formed from a cloud with fractal dimension $D = 2.8$.

We have, as yet, only considered a small part of the relevant parameter space. However, the morphological features of the HII regions generated by these simulations bear a striking resemblance to observed HII regions, with an abundance of bright arcs, bright rims and elephants' trunks. A fuller report on these results is in preparation but Figure 1 gives a first impression. The morphology of RCW 79 (Fig.1, righthand frame), a region where the collect and collapse process seems to be responsible for triggering star formation, can be well matched with a model of an HII region expanding into a rather uniform cloud, where bright rims and trunks dominate the final picture.

## References

Bisbas, T. G., Wünsch, R., Whitworth, A. P., & Hubber, D. A. 2009, *A&A*, 497, 649

Churchwell, E., Whitney, B. A., & Babler, B. L., *et al.* 2004, *ApJS*, 154, 322

Deharveng, L., Zavagno, A., Schuller, F., Caplan, J., Pomarès, M., & De Breuck, C. 2009, *A&A*, 496, 177

Zavagno, A., Deharveng, L., Comerón, F., Brand, J., Massi, F., Caplan, J., & Russeil, D. 2006, *A&A*, 446, 171

Hubber, D. A., Batty, C. P., McLeod, A., & Whitworth, A. P. 2010, submitted to *MNRAS*

Kauffmann, J., Pillai, T., Shetty, R., Myers, P. C., & Goodman, A. A. 2010, *ApJ*, 716, 433

Koenig, X. P., Allen, L. E., Gutermuth, R. A., Hora, J. L., Brunt, C. M., & Muzerolle, J. 2008, *ApJ*, 688, 1142

Larson, R. B. 1981, *MNRAS*, 194, 809

Stutzki, J., Bensch, F., Heithausen, A., Ossenkopf, V., & Zielinsky, M. 1998, *A&A*, 336, 697

Smith, N., Povich, M. S., Whitney, B. A., Churchwell, E., Babler, B. L., Meade, M. R., Bally, J., Gehrz, R. D., Robitaille, T. P., & Stassun, K. G. 2010, *MNRAS*, in press